Cancer Letters 446 (2019) 49–61

Contents lists available at ScienceDirect

Cancer Letters

journal homepage: www.elsevier.com/locate/canlet

Original Articles

Silencing of long noncoding RNA LINC00958 prevents tumor initiation of pancreatic cancer by acting as a sponge of microRNA-330-5p to down-regulate PAX8

Shi Chen[a,b,1], Jiang-Zhi Chen[c,1], Jia-Qiang Zhang[b,1], Hui-Xing Chen[c], Fu-Nan Qiu[a], Mao-Lin Yan[a], Yi-Feng Tian[a], Cheng-Hong Peng[b], Bai-Yong Shen[b,*], Yan-Ling Chen[c,**], Yao-Dong Wang[a,***]

[a] Department of Hepatobiliary Surgery, Fujian Provincial Hospital, Fujian Medical University, Fuzhou, 350001, PR China
[b] Pancreatic Disease Center, Department of General Surgery, Ruijin Hospital Affiliated to Shanghai Jiaotong University School of Medicine, Shanghai, 200025, PR China
[c] Department of Hepatobiliary Surgery, Union Hospital, Fujian Medical University, Fuzhou, 350001, PR China

ARTICLE INFO

Keywords:
Long noncoding RNA LINC00958
microRNA-330-5p
PAX8LINC00958/miR-330-5p/PAX8axis
Pancreatic cancer
Epithelial-mesenchymal transition
Invasion
Metastasis

ABSTRACT

Pancreatic cancer (PC) represents a relatively rare but severe malignancy worldwide. Accumulated studies have emphasized the potential of long noncoding RNA (lncRNA) as therapeutic strategies for several human cancers. Thus, we aimed to investigate whether a novel non-coding RNA regulatory circuitry involved in PC. Aberrantly expressed lncRNAs and mRNAs were screened out of microarray database. Following the determination of RNA expression, PANC-1 and BxPC-3 PC cells were adopted, after which the expression of miR-330-5p, PAX8 and LINC00958 were subsequently altered. RNA crosstalk was validated by dual-luciferase reporter gene assay. In order to detect whether LINC00958 could act as ceRNA to competitively sponge miR-330-5p and regulate PAX8, subcellular location of LINC00958 and interaction between LINC00958 and miR-330-5p were measured by FISH and RNA pull down respectively. The epithelial mesenchymal transition (EMT) process, cell invasion, and tumor growth were determined *in vitro* and *in vivo*. LINC00958 and PAX8 were up-regulated, while miR-330-5p was down-regulated during PC. LINC00958 mainly expressed in the cytoplasm and LINC00958 competitively sponged miR-330-5p. Upregulated miR-330-5p or downregulated PAX8 inhibited the EMT process as well as the invasion and metastasis ability of the PC cells. Moreover, the results indicated that miR-330-5p negatively targeted PAX8, and LINC00958 ultimately showcasing its ability to bind to miR-330-5p through its interaction with AGO2. Therefore, silencing of LINC00958 may bind to miR-330-5p to inhibit PAX8 in a competitive fashion, thereby preventing the progression of PC.

1. Introduction

As a relatively rare tumor representing the fourth most common cause of cancer mortality globally, pancreatic cancer (PC) results in approximately 227 000 deaths annually worldwide [1,2]. PC is often accompanied by a very poor prognosis, with nearly all PC patients dying within 7 years of surgery [3]. Studies have revealed there to be several risk factors involved in the incidence of PC, including that of smoking, chronic pancreatitis, long-standing diabetes, and somatic mutations, among which, that of smoking has been indicated to be the most universal, directly accounting for approximately 20–25% of all pancreatic tumors [4]. A large and progressively growing body of literature has indicated there to be limited diagnostic biomarkers available in regard to the imaging technologies and conventional serum biomarkers for PC owing to restricted sensitivity and specificity [5], all of which contribute to the overall 5-year survival rate among PC patients being less than 5% [6]. As a result, it is an absolute necessity that novel therapeutic targets are identified in order to aid in the diagnosis

* Corresponding author. Pancreatic Disease Center, Department of General Surgery, Ruijin Hospital Affiliated to Shanghai Jiaotong University School of Medicine, No. 197, Ruijin No. 2 Road, Shanghai, 200025, PR China.
** Corresponding author. Department of Hepatobiliary Surgery, Union Hospital, Fujian Medical University, No. 29, Xinquan Road, Fuzhou, 350001, Fujian Province, PR China.
*** Corresponding author. Department of Hepatobiliary Surgery, Fujian Provincial Hospital, Fujian Medical University, No. 134, East Street, Fuzhou, 350001, Fujian Province, PR China.
E-mail addresses: shenby@shsmu.edu.cn (B.-Y. Shen), drchenyl@126.com (Y.-L. Chen), wangyaodongch@163.com (Y.-D. Wang).
[1] These authors contributed equally to this work.

https://doi.org/10.1016/j.canlet.2018.12.017
Received 11 July 2018; Received in revised form 13 November 2018; Accepted 16 December 2018

and treatment of PC.

Accumulating evidence has demonstrated there to be a close association between long noncoding RNAs (lncRNAs), a class of RNA with transcripts longer than 200 nucleotides, and the processes of proliferation, metastasis, tumorigenesis, diagnosis and prognosis of various human cancers, such as prostate cancer, glioma [7–9]. Previous studies have provided evidence suggesting that the upregulation of lncRNAs participate in the incidence and progression of PC, including that of urothelial carcinoma-associated 1 (UCA1), metastasis-associated lung adenocarcinoma transcript 1 (MALAT-1), HOXA distal transcript antisense RNA (HOTTIP)-005, and RP11-567G11.1 [10–12]. More specifically, lncRNAs have been noted to possess an array of functions in relation to PC cell growth, differentiation, proliferation, invasion, metastasis, and apoptosis [13]. In recent years, long intergenic noncoding RNA 00958 (LINC00958) has been identified as an oncogenic gene in human cancers [8]. Seitz et al. earmarked LINC00958 as a potential biomarker for bladder cancer by binding proteins involved in regulating and initiating translation and in post-transcriptionally modifying RNA [14]. In addition, studies have revealed that microRNA-146b-5p (miR-146b-5p) to be a potential target for PC regarding its participation in the migration and invasion of PC cells by targeting matrix metallopeptidase 16 (MMP16) [15]. MiRs are small non-coding RNA molecules, that serve as regulators in the inhibition of messenger RNA (mRNA) translation or reduction of mRNA stability by binding the 3′ untranslated region (3'UTR) of target mRNA [16,17]. MiR-330-5p in particular has been reported to act as a tumor suppressor by means of its role in the progression of prostate, neuronal and pancreatic cancers by regulating proliferation, migration, invasion and epithelial-mesenchymal transition of cells [18,19]. Paired box(PAX) genes that encode a family of transcription factors significant for organogenesis, have been emphasized on in recent literature as potential immunohistochemical biomarkers for pancreatic neuroendocrine tumors [20]. For example, PAX8 gene encodes for a transcription factor, which exerts significant impacts on the development of epithelial organ structures [21]. What's more, it has been reported that PAX8 plays a pivotal role in thyroid cancer [22]. Based on the exploration of literature, the present study subsequently set out to explore the modulatory effects of the LINC00958/miR-330-5p/PAX8 axis on the progression of PC.

2. Materials and methods

2.1. Ethics statement

This study was conducted with the approval of the Ethics Committee of Ruijin Hospital Affiliated to Shanghai Jiaotong University School of Medicine, the Ethics Committee of Fujian Provincial Hospital, Fujian Medical University and the Ethics Committee of Union Hospital, Fujian Medical University.

2.2. Profiling data analysis

The GEO database (https://www.ncbi.nlm.nih.gov/geo/) was employed for bioinformatics prediction purposes. PC chip data (GSE27890) and annotate probe files were downloaded. The Affy installation package of R software was used to conduct the background correction and normalization of each chip data [23]. Next, the Linear Models and Empirical Bayes Methods of Limma installation package were applied and combined in connection with a traditional *t*-test in order to conduct a nonspecific filtration process for gene expression profiling, followed by screening out the differentially expressed long noncoding RNA and mRNA [24]. Finally, the RNA22 website (https://cm.jefferson.edu/rna22/) was used to verify miRNAs that combined with lncRNA and mRNA, while the RNA22 website combined with TCGA (http://cancergenome.nih.gov/) database was explored to download information about the prognosis and genes expression of PC. R software was employed to analyze the correlation of PC with PAX8. Differential analysis was performed for the transcriptome profiling data with package edgeR of R [25]. False positive discovery (FDR) correction was applied based on the p-value with package multitest. FDR < 0.05 and $|\log2 \text{ (fold change)}| > 2$ were set as the threshold to screen out differentially expressed genes (DEGs). Next, Kaplan-Meier survival curves were constructed in order to estimate the overall survival time for patients with predicted high- or low-expression group and the survival differences between high-expression group and low-expression group were assessed by a two-sided log-rank test using the R package "survival" [26]. Hazard ratio (HR) and 95% confidence intervals (CI) were estimated by means of a Cox proportional hazards regression model.

2.3. Cell treatment

Human PC cell lines PANC-1, Capan-2, SW1990, and BxPC-3 and human normal pancreatic ductal epithelial cell line HPDE were purchased from American Type Culture Collection (ATCC, Manassas, VA, USA). The culture condition of the above cell lines were as follows: HPDE: Kerationcyte-SFM medium (10724-011, Gibco Company, Grand Island, NY, USA) + 0.1 μg/L epidermal growth factor (EGF) + 25 mg/L bpe [27]; PANC-1: dulbecco modified eagle medium (DMEM) medium + 10% fetal bovine serum (FBS) + 1% penicillin/streptomycin (Beyotime Biotechnology Co., Ltd., Shanghai, China); Capan-2 and BxPC-3: Roswell Park Memorial Institute (RPMI)1640 medium + 10% FBS + 1% penicillin/streptomycin (Beyotime Biotechnology Co., Ltd., Shanghai, China); SW1990: RPMI1640 medium + 10% FBS + 1% penicillin/streptomycin (Beyotime Biotechnology Co., Ltd., Shanghai, China) + Leibovitz's L-15 (11415-064, Gibco Company, Grand Island, NY, USA) [28]. The cells were then seeded into a 6-well plate at a density of 4×10^5 cells/well and conventionally sub-cultured in a 5% CO_2 incubator with saturated air humidity at 37 °C.

Prior to transfection, the cells covered approximately 60% of the plates, with the culture medium in each well replaced with MEM culture medium (Gibco Company, Grand Island, NY, USA) without serum, penicillin, or streptomycin for 2 h culture. Next, 1.5 mL opti-MEM was added to the cells and pre-heated in an incubator. The plasmids, including miR-330-5p inhibitor, miR-330-5p mimic, and negative control (NC), purchased from Shanghai Novo Biotechnology Co., Ltd. (Shanghai, China), and PAX8 ORF, PAX8 siRNA, si-LINC00958, si-NC, pcDNA-LINC00958, as well as the empty vectors, purchased from Shanghai Genechem Co., Ltd. (Shanghai, China), Opti-MEM and Lipectamine® 2000 transfection reagent (Invitrogen Inc., Carlsbad, CA, USA) were mixed in an even manner and permitted to stand for 5 min. The mixture was then added into PANC-1 and BxPC-3 cell culture medium, and mixed evenly. After incubation for 24 h, a fresh culture medium was added to the cells. After transfection for 48 h, the cells were detached with trypsin and collected for later experiments. The cells were then subsequently categorized into the blank group (without transfection), a NC group (transfected with si-NC plasmids of miR-330-5p), a miR-330-5p inhibitor group (transfected with miR-330-5p inhibitor plasmids), a miR-330-5p mimic group (transfected with miR-330-5p mimic plasmids), a PAX8 siRNA group (transfected with PAX8 siRNA plasmids), a PAX8 ORF group (transfected with PAX8 ORF plasmids), a miR-330-5p inhibitor + PAX8 siRNA group (transfected with miR-330-5p inhibitor plasmids and PAX8 siRNA plasmids) and a miR-330-5p mimic + PAX8 ORF group (transfected with miR-330-5p mimic and PAX8 ORF plasmids). Next, the cells were grouped into the blank group (without any treatment), a si-NC group (transfected with si-NC plasmids of LINC00958), a si-LINC00958 group (transfected with si-LINC00958 plasmids), an empty vector group (transfected with empty vectors), and a pcDNA-LINC00958 group (transfected with pcDNA-LINC00958 plasmids).

Table 1
Primer sequences of related genes for RT-qPCR.

Gene	Sequence (5'- 3')	
	Forward	Reverse
LINC00958	CCATTGAAGATACCACGCTGC	GGTTGTTGCCCAGGGTAGTG
miR-330-5p	TCTCTGGGCCTGTGTCTTAGGC	CAGTGCGTGTCGTGGAGT
PAX8	CGGCAACGCATTGTGGA	TCCTGGGCTCAGAGATTTGC
U6	AGAGAGATTACATGGCCCCT	CTAATGTCACGCACGATTCT
GAPDH	GTCAACGGATTTGGTCTGTATT	AGTCTTCTGGGTGGCAGTGAAT

Note: RT-qPCR, reverse transcription quantitative polymerase chain reaction; LINC00958, long intergenic non-coding 00958; miR-330-5p, microRNA-330-5p; PAX8, paired box 8; GAPDH, glyceraldehyde-3-phosphate dehydrogenase.

2.4. RNA extraction and reverse transcription quantitative polymerase chain reaction (RT-qPCR)

The total RNA of the cells and tissues were extracted using a Trizol kit (16096020, Thermo Fisher Scientific Invitrogen, CA, USA). The total RNA (5 μg) was then reversely transcribed into cDNA by RT-qPCR kit (ABI Company, Oyster Bay, NY, USA) based on the instructions of the kit. The amplification of the target gene system using PROGENE PCR amplification instrument (Techene, London, UK) was comprised of 25 μL. The reaction system was set as follows: 300 ng cDNA, 1 × PCR buffer, 200 μmol/L dNTPs, 80 pmol/L forward primer, 80 pmol/L reverse primer, and 0.5 U Taq enzyme (S10118, Shanghai yuanye Bio-Technology Co., Ltd., Shanghai, China). Reaction conditions were as follows: 30 cycles of pre-denaturation at 94 °C for 5 min, denaturation at 94 °C for 30 s, annealing at 54.5 °C for 30 s, and extension at 72 °C for 10 min, and elongation at 72 °C for 10 min. The samples were then preserved at 4 °C. The primer sequences of miR-330-5p, U6, PAX8, glyceraldehyde-3-phosphate dehydrogenase (GAPDH), LINC00958 are depicted in Table 1. U6 was regarded as the internal reference of miR-330-5p, while GAPDH considered to be the internal reference of other genes. The ratio of relative target gene expression between the experiment group and the control group was analyzed by $2^{-\Delta\Delta Ct}$ method, the formula of which was as follows: $\triangle\triangle Ct = \triangle Ct_{\text{experimental group}} - \triangle Ct_{\text{control group}}$, $\triangle Ct = Ct_{\text{target gene}} - Ct_{\text{internal reference}}$. Ct represented the amplification cycles when real-time fluorescence intensity reached threshold at reaction, during which the amplification exhibited logarithmic growth. The experiment was repeated three times.

2.5. Dual-luciferase reporter gene essay

Target gene analysis of miR-330-5p was performed using the biological prediction website Targetscan.org, while a dual-luciferase reporter gene assay was applied in order to ascertain as to whether PAX8 was indeed a direct target gene of miR-330-5p. The artificially synthesized PAX8 3′UTR gene fragment was inserted into pMIR-reporter using enzyme sites SpeI and Hind III (Beijing, Huayueyang Biotechnology, Beijing, China). The mutant (Mut) sites of supplementary sequences of seed sequences were designed in PAX8 wild type (Wt). After restriction endonuclease digestion, the T4 DNA ligase was used to insert the target fragments into the pMIR-reporter plasmids. The correctly identified luciferase reporter plasmids Wt and Mut were then co-transfected into HEK-293T cells (Shanghai Beinuo Biotechnology, Co., Ltd., Shanghai, China) with miR-330-5p, respectively. After transfection for 48 h, the cells were collected and split, while the luciferase assay kit (K801-200, BioVision. Inc., SF, USA), and Glomax20/20 luminometer luciferase instrument (Promega Corp., Madison, Wisconsin, USA) were employed to detect luciferase activity. The experiment was repeated three times.

Next, the biological prediction website was used to analyze the binding relationship between LINC00958 and miR-330-5p, while a dual-luciferase reporter gene assay was utilized to verify that miR-330-5p was the direct target of LINC00958. miR-330-5p 3′UTR gene fragment was artificially synthesized and then inserted into pMIR-reporter using enzyme sites SpeI and Hind III (Beijing, Huayueyang Biotechnology, Beijing, China). The Mut sites of supplementary sequences of seed sequences were designed in miR-330-5p Wt. After restriction endonuclease digestion, the target fragments were inserted into the pMIR-reporter plasmids by the T4 DNA ligase. The correctly sequenced luciferase reporter plasmids Wt and Mut were co-transfected with LINC00958 into HEK-293T cells (Shanghai Beinuo Biotechnology, Co., Ltd., Shanghai, China). After 48-h transfection, the cells were collected and split, and luciferase activity was detected by Glomax® 20/20 luminometer luciferase instrument (Promega Corp., Madison, Wisconsin, USA). The experiment was repeated three times.

2.6. Western blot analysis

After transfection, cells in each group were washed twice with PBS, followed by treatment with radio-immunoprecipitation assay (RIPA) lysis buffer (P0013B, Beyotime Biotechnology Co., Ltd., Shanghai, China), and shaken on a swirl instrument. The samples were then centrifuged at a rate of 12000 r/min at 4 °C for 30 min allowing for the removal of cell fragments, followed by the extraction of the cell supernatant. The total protein concentration was measured using a bicinchoninic acid (BCA) kit. The protein (50 μg) was extracted and dissolved in 2 × sodium dodecyl sulfate (SDS) loading buffer and boiled at 100 °C for 5 min. Next, the samples were treated with 10% SDS- polyacrylamide gel electrophoresis (PAGE), and transferred onto a polyvinylidene fluoride (PVDF) membrane using the wet transfer method. Then, the membrane was blocked in 5% skimmed milk powder for 1 h at room temperature. The membrane was incubated with diluted primary antibodies rabbit anti-human β-actin (1: 100, ab8224, Abcam Inc., Cambridge, MA, USA), mouse monoclonal antibody E-cadherin (1: 1000, ab76055, Abcam Inc., Cambridge, MA, USA), mouse monoclonal antibody vimentin (1: 2000, ab8978, Abcam Inc., Cambridge, MA, USA), rabbit polyclonal antibody matrix metallopeptidase 2 (MMP-2) (1: 10000, ab37150, Abcam Inc., Cambridge, MA, USA), rabbit polyclonal antibody matrix metallopeptidase 9 (MMP-9) (1: 10000, ab38898, Abcam Inc., Cambridge, MA, USA) overnight. Next, the membrane was rinsed with tris-buffered saline and Tween 20 (TBST; BOSTER Biological Technology Co. Ltd., Wuhan, Hubei, China) three times, followed by culturing with horseradish peroxidase (HRP)-labeled secondary antibody (1: 5000, Abcam Inc., MA, USA) for 1 h. After rinsing with TBST, the membrane was placed on a clean glass plate. An equal amount of A solution and B solution from electro-chemi-luminescence (ECL) kit (BB-3501, Amersham, Arlington Heights, IL, USA) was extracted and mixed evenly under dark conditions, followed by the addition of the mixture to the membrane, which was exposed and imaged on a gel imaging instrument. The membrane was photographed by Bio-rad Gel Dol EZ gel imaging instrument (Bio-Rad, Hercules, CA, USA), and analyzed by Quantity One v4.6.2. The relative protein levels were expressed as gray value ratio of target protein band to the internal reference band. The experiment was repeated three times.

2.7. Immunofluorescence assay

The transfected cells were then seeded into a 24-well plate precoated with polylysine. After cell adherence was observed, the culture medium was abandoned, followed by washing of the cells with prewarm PBS (0.01 mol/L) three times, and fixation with 4% polyoxymethylene at room temperature for 30 min. After 3 additional PBS (0.01 mol/L) washes (10 min per wash), the blocking buffer (Beyotime Biotechnology Co., Ltd., Shanghai, China) was added prior to 60-min of incubation at 37 °C. After solution removal, the samples were incubated with mouse monoclonal antibody E-cadherin (ab76055, Abcam Inc., Cambridge, MA, USA), and mouse monoclonal antibody vimentin (ab8978, Abcam Inc., Cambridge, MA, USA) at 4 °C overnight. The

samples were then washed 3 times with PBS (0.01 mol/L) (10 min per wash), followed by incubation with fluorescence secondary antibody Alexa Fluor 594 donkey anti-rabbit (1: 400, A21202, Thermo Fisher Scientific Inc., Waltham, MA, USA)/Alexa Fluor 488 donkey anti-mouse (1: 400, A21207, Thermo Fisher Scientific Inc., Waltham, MA, USA) under conditions void of light for 1 h, and stained with 4′,6-diamidino-2-phenylindole (DAPI) (Beyotime Biotechnology Co., Ltd., Shanghai, China) at room temperature for 5 min. The samples were subsequently added with an appropriate amount of anti-fluorescence quenching mounting medium (Beyotime Biotechnology Co., Ltd., Shanghai, China), imaged and photographed using molecular devices high content screening. The molecular device metaxpress image acquisition and analysis software were applied to evaluate the module for statistical analysis purposes. The experiment was repeated three times.

2.8. Transwell assay

The surface of filter membrane of transwell chamber (8 μm, Sigma-Aldrich Chemical Company, St Louis MO, USA) was covered with the Matrigel membrane (Sigma-Aldrich Chemical Company, St Louis MO, USA), and placed in a 24-well plate. The transfected cells in each group and cancer cell suspension of obtained from each nude mouse among all groups (200 μL, 1×10^5 cells/mL) were added to the apical chamber. Next, the 10% FBS (600 μL) was added into the basolateral region of the chamber. After 24 h incubation in a 5% CO_2 incubator at 37 °C, the liquid in the apical chamber was removed. The cells yet to be transferred as well as the matrigel in the apical chamber were wiped off using cotton buds. The basolateral chamber was fixed in methanol for 10 min, followed by staining with hematoxylin-eosin (HE). The cells that were observed to have migrated into the lower level of microporous membrane were counted and photographed under an inverted microscope. Next, 5–10 visual fields were selected in each group. Image-pro Plus software was employed to record the number, with each group undergoing three repeats in order to obtain the mean value.

2.9. Tumorigenicity assay in nude mice

A total of 30 athymic female nude mice (age: 4–6 weeks old, weight: about 20 g) purchased from the Animal Center of the Institute of Cancer Research in Chinese Academy of Medical Sciences (Beijing, China) (Animal certificate number: Jing animal (certificate No.) 017), and were classified as PANC-1 and BxPC-3 cells, with three subgroups in each group ($n = 5$). Next, the NC, miR-330-5p inhibitor, and miR-330-5p mimic were transfected into PC cells. The concentration of the transfected cells in the logarithmic growth phase was adjusted into $4 \times 10^5\ mL^{-1}$. The cell suspension (0.1 mL) was subcutaneously injected into the back of the nude mice based on the respective establishment of tumor xenograft model among the nude mice in each group. After a week, the tumor volume of the nude mice was measured once every three days, and a vernier caliper was used to measure the length (a) and width (b) to calculate the tumor volume, tumor volume = $a \times b^2/2$. The period of experiment was 21 days. At the end of experiment, all nude mice were sacrificed by CO_2, and the tumor was isolated and weighed. The mean tumor volume of nude mice in each group was subsequently determined. The liver of nude mice was extracted, fixed in 4% polyoxymethylene, and stained with HE for pathological analysis purposes, which was conducted in accordance with the instructions of HE kit (Beyotime Biotechnology Co., Ltd., Shanghai, China) [29]. All of the experimental procedures were carried out in accordance with the institution's guidelines for the care and use of laboratory animals.

2.10. RNA immunoprecipitation (RIP)

An RIP kit (Merck KGaA, Darmstadt, Germany) was utilized to detect the binding of LINC00958 protein with AGO. The PC PANC-1 cells were washed with pre-cooled PBS followed by discarding of the cell supernatant. The cells were then split after the addition of an equal amount of RIPA lysate and 5-min ice bath. The cells were then centrifuged at 14000 rpm at 4 °C for 10 min to collect the supernatant. A portion of the cell extract was isolated as the Input, while the other portion was incubated with an antibody for co-precipitation. Each co-precipitation reaction system (50 μL) was washed with magnetic beads, and resuspended in 100 μL RIP Wash Buffer. The antibody (5 μg) was added to the samples according to the groups and incubated for binding. After rinsing, the bead-antibody complex was resuspended in RIP Wash Buffer (900 μL), followed by the addition of the cell extract (100 μL) to the samples and incubation at 4 °C overnight. The samples were then placed on the beads in order to collect the bead-antibody complex. The samples and Input were treated with protease K for RNA extraction and subsequent PCR detection. The antibody used in RIP was rabbit anti-mouse AGO2 (ab186733, 1: 50, Abcam Inc., Cambridge, MA, USA), and mixed with samples at room temperature for 30 min. The rabbit anti-mouse IgG (ab109489, 1: 100, Abcam Inc., Cambridge, MA, USA) served as the negative control.

2.11. Fluorescent in Situ Hybridization (FISH)

FISH was performed for subcellular localization of LINC00958. The experiment was conducted according to the instructions of Ribo™ lncRNA FISH Probe Mix (Red) (RiboBio Co., Ltd., Guangdong, China). The cover glasses were placed into a 24-well plate and cells were inoculated at the density of 6×10^4 cells/well. When cell confluence reached 80%, the cover glasses were took out, and the cells were washed by PBS and fixed with 1 mL 4% paraformaldehyde at room temperature. After treatment with protease K, glycine and acetylation reagent, the cells were added with 250 μL prehybridization solution and incubated at 42 °C for 1 h. After prehybridization solution was discarded, the cells were added with 250 μL hybridization solution containing probe LINC00958 (300 ng/mL) for overnight hybridization at 42 °C. Then the cells were rinsed by phosphate buffered saline with tween-20 (PBST) 3 times, added with PBST-diluted DAPI dye liquor (ab104139, 1: 100, Abcam Inc., Cambridge, MA, USA) and placed into the 24-well plate for 5-min staining. Subsequently, the cells were washed by PBST 3 times (3 min per wash), sealed with anti-fluorescence quencher, observed and photographed under a fluorescence microscope (Olympus, Tokyo, Japan).

2.12. RNA pull down

The cells were transfected with 50 nM biotin-labeled Bio-probe NC, Bio-RNA LINC00958-Wt and Bio-RNA LINC00958-Mut. After 48 h, the cells were collected, rinsed by PBS, and incubated in specific lysis buffer (Ambion, Austin, Texas, USA) for 10 min. Lysates were incubated with M-280 streptavidin magnesphere (S3762, Sigma, St. Louis, MO, USA) pre-coated with RNase-free bovine serum albumin (BSA) and yeast tRNA (TRNABAK-RO, Sigma, St. Louis, MO, USA) in advance. After incubated at 4 °C for 3 h, the beads were washed with precooled lysis buffer twice, low salt buffer 3 times and high salt buffer once. The binding RNA was purified through Trizol, and RT-qPCR was conducted to detect the enrichment of miR-330-5p.

2.13. Statistical analysis

All experimental data was analyzed using SPSS 21.0 software (IBM Corp. Armonk, NY, USA). Measurement data with normal distribution were expressed as mean ± standard deviation, while mean value comparisons between two groups were analyzed using *t*-test. Enumeration data was expressed by percentage (%). Comparisons between two groups were analyzed using *t*-test. Measurement data comparisons among multiple groups were analyzed by means of one-way analysis of variance (ANOVA). Enumeration data were expressed by

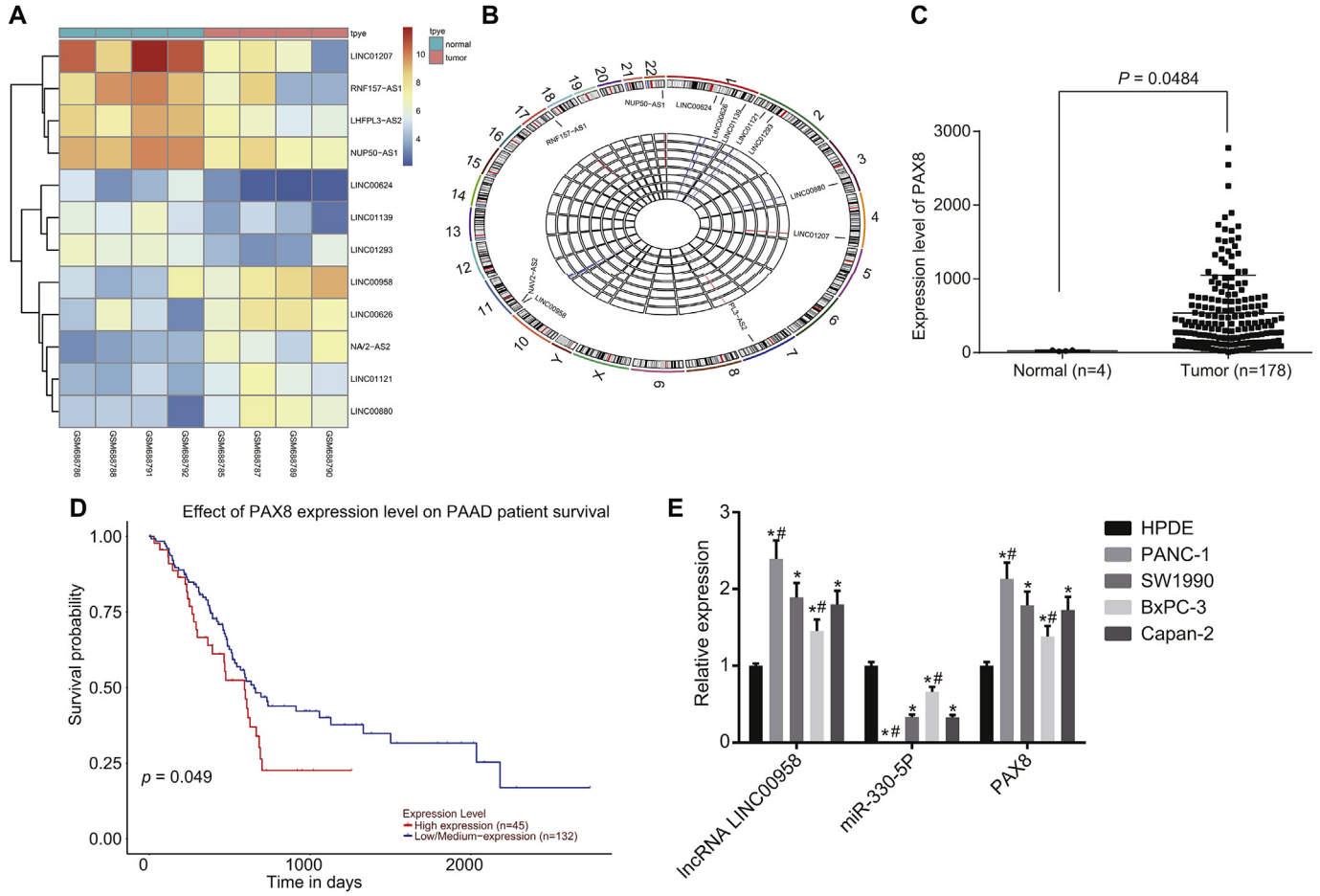

Fig. 1. LINC00958 and PAX8 are upregulated and miR-330-5p is downregulated in PC cells. A, a heat map of chip data GSE27890 analysis; B, a Circos map of chip data GSE27890; C, PAX8 expression in PC through TCGA database; D, survival circle of PAX8 in the TCGA database; E, expression of LINC00958, miR-330-5p, and PAX8 in PC cell lines; the experiment was repeated 3 times and the results were analyzed using one-way analysis of variance; the measurement data were expressed as mean ± standard deviation; *, $p < 0.05$, compared with the HPDE cell line; $^{\#}$, $p < 0.05$, compared with the SW1990 and Capan-2 cell lines; PC, pancreatic cancer; miR-330-5p, microRNA-330-5p; TCGA, the cancer genome atlas; LINC00958, long intergenic non-coding 00958.

case number (percentage) and analyzed by *chi*-square test. $p < 0.05$ was considered to be statistically significant.

3. Results

3.1. LINC00958 and PAX8 express at high levels and miR-330-5p at low level in PC cells

Initially, in order to ascertain as to whether LINC00958, PAX8, and miR-330-5p were suitable for the experiment, bioinformatics predictions were conducted. Evaluation of the gene expression profile (GSE27890) of PC, revealed that LINC00958 was the most significantly upregulated long non-coding RNA in PC (Fig. 1A and B). The RNA22 website revealed that LINC00958 could bind to miR-330-5p in order to regulate PAX8 expression. Moreover, the TCGA database further verified that PAX8 was highly activated in PC cells (Fig. 1C), as well as highlighting its association with the prognosis of PC (Fig. 1D). RT-qPCR was then performed in order to determine the expression of LINC00958, miR-330-5p, as well as PAX8 among the PC cell lines, the findings of which indicated that compared with the HPDE, the expression of LINC00958 and PAX8 was markedly increased in the PC cell lines, while the levels of miR-330-5p were evidently reduced (all $p < 0.05$). Additionally, in PANC-1 cell line, LINC00958 and PAX8 showed the highest expression while miR-330-5p showed the poorest expression; in BxPC-3 cell line, LINC00958 and PAX8 displayed the poorest expression, while that of miR-330-5p exhibited the highest expression, which was in significant contrast to the SW1990 and Capan-2 cell lines (all $p < 0.05$). As a result of the obtained results, PANC-1 and BxPC-3 cell lines were selected to investigate the effects involved with the miR-330-5p/PAX8 axis on EMT, invasion, and metastasis of PC cells (Fig. 1E).

3.2. PAX8 is a target gene of miR-330-5p

Next, in order to identify the targeting effect of miR-330-5p on PAX8, the website http://www.targetscan.org as well as a dual-luciferase reporter gene assay were employed, the results of which indicated that in PANC-1 and BxPC-3 cell lines, when compared with the NC group, luciferase activity of Wt PAX8 3′-UTR was significantly inhibited by miR-330-5p mimic ($p < 0.05$), however no significant difference was observed in Mut PAX8 3′-UTR ($p > 0.05$). Taken together, a conclusion that miR-330-5p could bind with PAX8-3′-UTR and downregulate PAX8 expression was subsequently made (Fig. 2A, B, D).

In order to further elucidate the means by which miR-330-5p targets PAX8, PANC-1 and BxPC-3 cell lines were transfected with NC, miR-330-5p inhibitor, and miR-330-5p mimic plasmids. With the blank group as the control, RT-qPCR was performed to measure the PAX8 expression in PANC-1 and BxPC-3 cell lines in the blank, NC, miR-330-5p inhibitor, and miR-330-5p mimic groups. The findings demonstrated there was significant difference in PAX8 expression between the blank and NC groups ($p > 0.05$), while the miR-330-5p inhibitor group exhibited elevated levels of PAX8 expression, with the result in the miR-330-5p mimic group exhibiting an opposite trend (both $p < 0.05$).

A

	Predicted consequential pairing of target region (top) and miRNA(bottom)	Site type	Context++ score
Position 135-142 of PAX8 3' UTR	5' ...CAGCCUGGGACAGGC-CCCAGAGA...	8mer	-0.17
hsa-miR-330-5p	3' CGGAUUCUGUGUCCGGGGUCUCU		

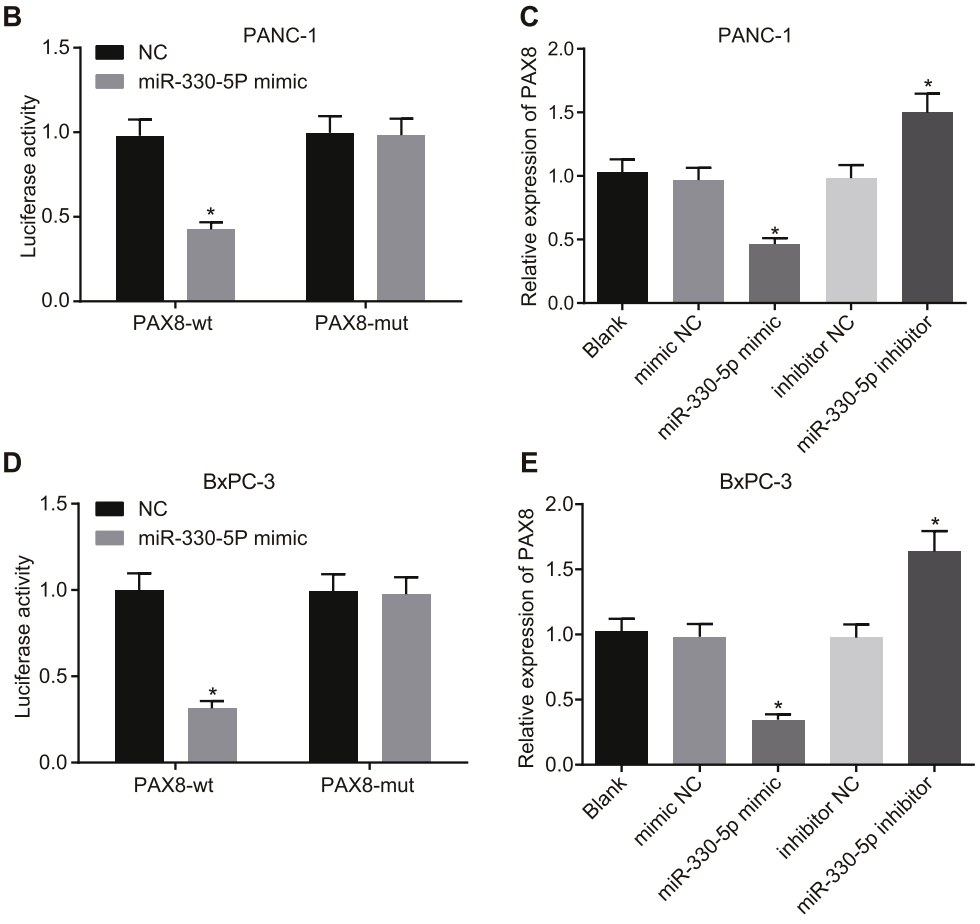

Fig. 2. miR-330-5p targets and negatively regulates PAX8. A, prediction binding site of miR-330-5p in PAX8 3′UTR; B&C, detection of luciferase activity and PAX8 mRNA expression in PANC-1 cell line; D&E, detection of luciferase activity and PAX8 mRNA expression in BxPC-3 cell line; the experiments were repeated 3 times and the results of which were analyzed by using non-paired *t*-test; the measurement data were expressed as mean ± standard deviation; *, $p < 0.05$, compared with the mimic NC group or inhibitor NC group; Wt, wild type; Mut, mutant type; NC, negative control; miR-330-5p, microRNA-330-5p; PAX8, paired box 8; LINC00958, long intergenic non-coding 00958.

Compared with the miR-330-5p inhibitor group, PAX8 expression was downregulated in the miR-330-5p mimic group ($p < 0.05$). Taken together, the obtained findings revealed that miR-330-5p negatively targets PAX8 (Fig. 2C, E).

3.3. Up-regulation of miR-330-5p or silencing PAX8 inhibits EMT of PC cells

In order to explore the effects of miR-330-5p/PAX8 axis on EMT of PC cells, an immunofluorescence assay and western blot analysis were both adopted in order to detect the protein levels of E-cadherin, and vimentin in PANC-1 and BxPC-3 cells in each group after transfection. Results of immunofluorescence assay showed that in PANC-1 and BxPC-3 cells, E-cadherin was determined to be expressed in cell membrane and cytoplasm, and mainly distributed in membrane, while vimentin was expressed in cytoplasm (Fig. 3A and B). Results of western blot analysis displayed that compared with the blank group, the protein levels of E-cadherin and vimentin presented no significant difference in the NC, miR-330-5p inhibitor + PAX8 siRNA and miR-330-5p mimic + PAX8 ORF groups (all $p > 0.05$). Compared with the blank, NC, and miR-330-5p inhibitor + PAX8 siRNA groups, the miR-330-5p inhibitor and PAX8 ORF groups displayed evidently reduced levels of E-cadherin protein as well as increased protein level of vimentin (all $p < 0.05$), while the miR-330-5p mimic and PAX8 siRNA groups displayed a contrasting result (all $p < 0.05$). Significant differences in relation to the protein levels of E-cadherin and vimentin in the miR-330-5p inhibitor + PAX8 siRNA group in comparison to the miR-330-5p inhibitor, PAX8 siRNA and miR-330-5p mimic + PAX8 ORF groups were detected (all $p < 0.05$) (Fig. 3C,D, E, F). These results indicated that silencing miR-330-5p could act to promote the EMT of PC cells, while the upregulation of miR-330-5p or downregulation of PAX8 may suppress the EMT of PC cells.

3.4. Up-regulation of miR-330-5p or silencing PAX8 inhibits the invasion and metastasis of PC cells

To investigate the effects of miR-330-5p/PAX8 axis on the invasion and metastasis of PC cells, a transwell assay was adopted in order to determine PC cell invasion, with a western blot analysis performed to assess the protein levels of MMP-2 and MMP-9 in PANC-1 and BxPC-3 cells in each group after transfection. According to results of transwell assay, regarding the PANC-1 and BxPC-3 cells, the cell invasion number presented no obvious difference in the blank, NC, miR-330-5p inhibitor + PAX8 siRNA and miR-330-5p mimic + PAX8 ORF groups (all $p > 0.05$). Compared with the blank, NC, and miR-330-5p inhibitor + PAX8 siRNA groups, increased cell invasion in the miR-330-5p inhibitor and PAX8 ORF groups were detected (all $p < 0.05$), while the miR-330-5p mimic and PAX8 siRNA groups displayed an opposite set of results (all $p < 0.05$). Significant differences were observed in relation to the cell invasion in the miR-330-5p

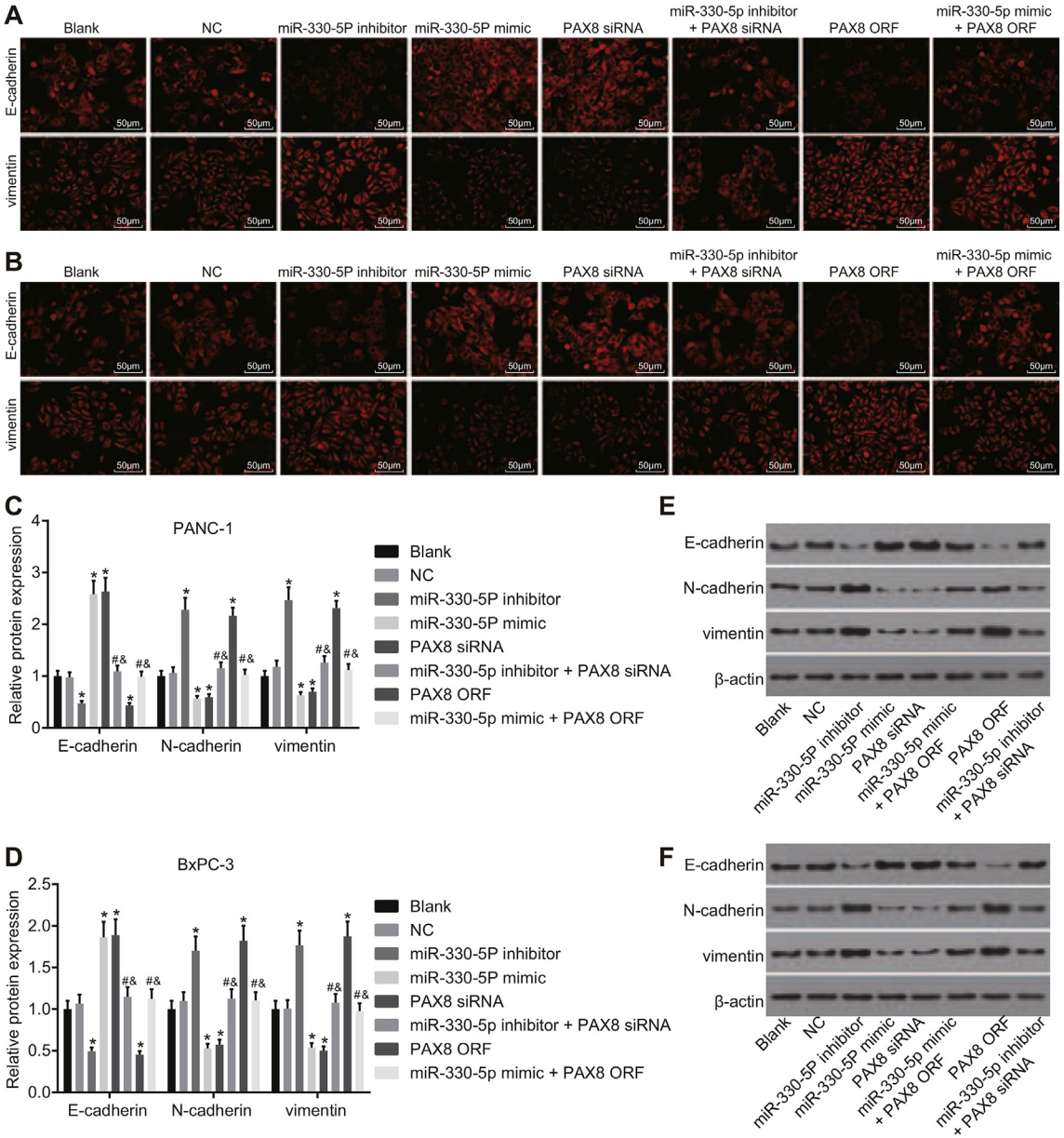

Fig. 3. miR-330-5p overexpression or silencing PAX8 inhibits EMT of PC cells. A, protein levels of E-cadherin and vimentin in PANC-1 cells using immunofluorescence assay (200 ×); B, protein levels of E-cadherin and vimentin in BxPC-3 cells using immunofluorescence assay (200 ×); C&D, protein levels of E-cadherin and vimentin in PANC-1 and BxPC-3 cells using western blot analysis; E&F, protein band patterns of E-cadherin and vimentin in PANC-1 and BxPC-3 cells using western blot analysis; the experiments were repeated 3 times with the results analyzed by using one-way analysis of variance; the measurement data were expressed as mean ± standard deviation; *, $p < 0.05$, compared with the blank group; $^{\#}$, $p < 0.05$, compared with the miR-330-5p inhibitor group; $^{\&}$, $p < 0.05$, compared with the PAX8 siRNA group; PC, pancreatic cancer; EMT, epithelial-mesenchymal transition; NC, negative control; miR-330-5p, microRNA-330-5p; PAX8, paired box 8; LINC00958, long intergenic non-coding 00958.

inhibitor + PAX8 siRNA and miR-330-5p mimic + PAX8 ORF groups in comparison to the miR-330-5p inhibitor group or the PAX8 siRNA group (all $p < 0.05$) (Fig. 4A, B, C).

Results of western blot analysis showed that in the PANC-1 and BxPC-3 cells, no obvious difference was found in levels of MMP-2 and MMP-9 in the blank, NC, miR-330-5p inhibitor + PAX8 siRNA and miR-330-5p mimic + PAX8 ORF groups (all $p > 0.05$). The miR-330-5p inhibitor and PAX8 ORF groups displayed higher levels of MMP-2 and MMP-9 while the miR-330-5p mimic and PAX8 siRNA groups showed lower levels of MMP-2 and MMP-9 than those in the blank, NC, and miR-330-5p inhibitor + PAX8 siRNA groups (all $p < 0.05$). There presented prominent differences in levels of MMP-2 and MMP-9 were found in the miR-330-5p inhibitor + PAX8 siRNA and miR-330-5p mimic + PAX8 ORF groups when compared with the miR-330-5p inhibitor group or the PAX8 siRNA group (all $p < 0.05$) (Fig. 4D, E, F, G). These results highlighted that silencing miR-330-5p could promote invasion and metastasis of PC cells, while the upregulation of miR-330-5p or downregulation of PAX8 could act to suppress invasion and metastasis of PC cells.

3.5. Up-regulation of miR-330-5p inhibits PC cell growth, invasion, and metastasis in nude mice

In order to explore the influence of miR-330-5p on the processes of cell growth, invasion, and metastasis of PC cells *in vivo*, PANC-1 and BxPC-3 cell mouse models were established in the NC, miR-330-5p inhibitor, and miR-330-5p mimic groups. Vernier caliper measurement and weighing method were applied to measure the tumor volume

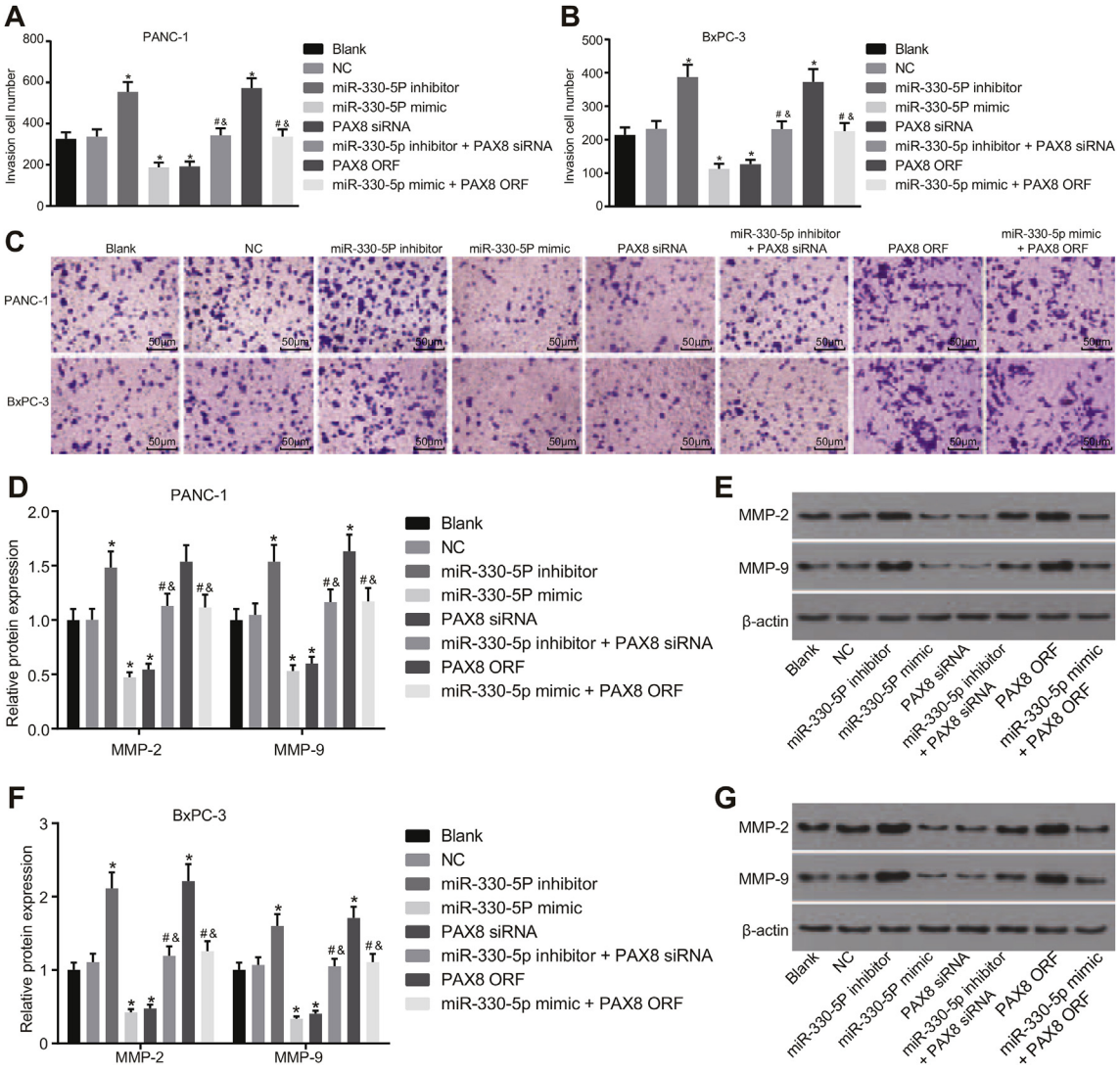

Fig. 4. miR-330-5p overexpression or silencing PAX8 inhibits invasion and metastasis of PC cells. A&B, the number of cell invasion in PANC-1 and BxPC-3 cells using transwell assay; C, transmembrane ability of PANC-1 and BxPC-3 cells using transwell assay (100 ×); D&E, protein levels and protein bands of MMP-2 and MMP-9 in PANC-1 cells using western blot analysis; F&G, protein levels and protein bands of MMP-2 and MMP-9 in BxPC-3 cells using western blot analysis; the experiments were repeated 3 times with the results analyzed by using one-way analysis of variance; the measurement data were expressed as mean ± standard deviation; *, $p < 0.05$, compared with the blank group; $^{\#}$, $p < 0.05$, compared with the miR-330-5p inhibitor group; $^{\&}$, $p < 0.05$, compared with the PAX8 siRNA group; PC, pancreatic cancer; NC, negative control; miR-330-5p, microRNA-330-5p; MMP, matrix metalloproteinase; PAX8, paired box 8; LINC00958, long intergenic non-coding 00958.

(Fig. 5A and B) and tumor weight (Fig. 5C, D, E) of nude mice in each group. After 13 days had elapsed, comparisons made to the NC group, revealed there to be a notably increased tumor volume and weight in miR-330-5p inhibitor group (both $p < 0.05$), while the miR-330-5p mimic group displayed reduced tumor volume and weight (both $p < 0.05$). Compared with the miR-330-5p inhibitor group, the miR-330-5p mimic group exhibited reduced tumor volume and weight (both $p < 0.05$). Besides, HE staining was performed to detect the number of metastatic nodules in the livers of the nude mice (Fig. 5F, G, H) and Western blot analysis was employed to determine the protein levels of MMP-2 and MMP-9 as well as EMT-related protein (N-cadherin, E-cadherin and vimentin) levels (Fig. 5I, J, K, L). The results revealed that compared with the NC group, the miR-330-5p inhibitor group revealed the elevated protein levels of MMP-2, MMP-9, N-cadherin and vimentin and increased number of liver metastatic nodules while reduced E-cadherin level (all $p < 0.05$), while the miR-330-5p mimic group displayed a contrasting trend (all $p < 0.05$). Compared with the miR-330-5p inhibitor, protein levels of MMP-2, MMP-9, N-cadherin and vimentin and the number of liver metastatic nodules were markedly decreased while E-cadherin level was increased in the miR-330-5p mimic group (all $p < 0.05$). The aforementioned findings suggested that silencing miR-330-5p could promote invasion and metastasis of PC cells in nude mice, while the upregulation of miR-330-5p or downregulation of PAX8 could suppress the invasion and metastasis of PC cells among nude mice.

3.6. Silencing LINC00958 inhibits EMT, invasion and metastasis of PC cells by suppressing miR-330-5p/PAX8 axis

Bioinformatics prediction was conducted to verify the relationship between LINC00958 and miR-330-5p. The results indicated that compared with the NC group, luciferase activity was suppressed when treated with Wt LINC00958-cDNA ($p < 0.05$), while the luciferase activity of Mut plasmids displayed no significant differences ($p > 0.05$), which indicated that LINC00958 could indeed bind with miR-330-5p. In addition, RIP was adopted to confirm the whether

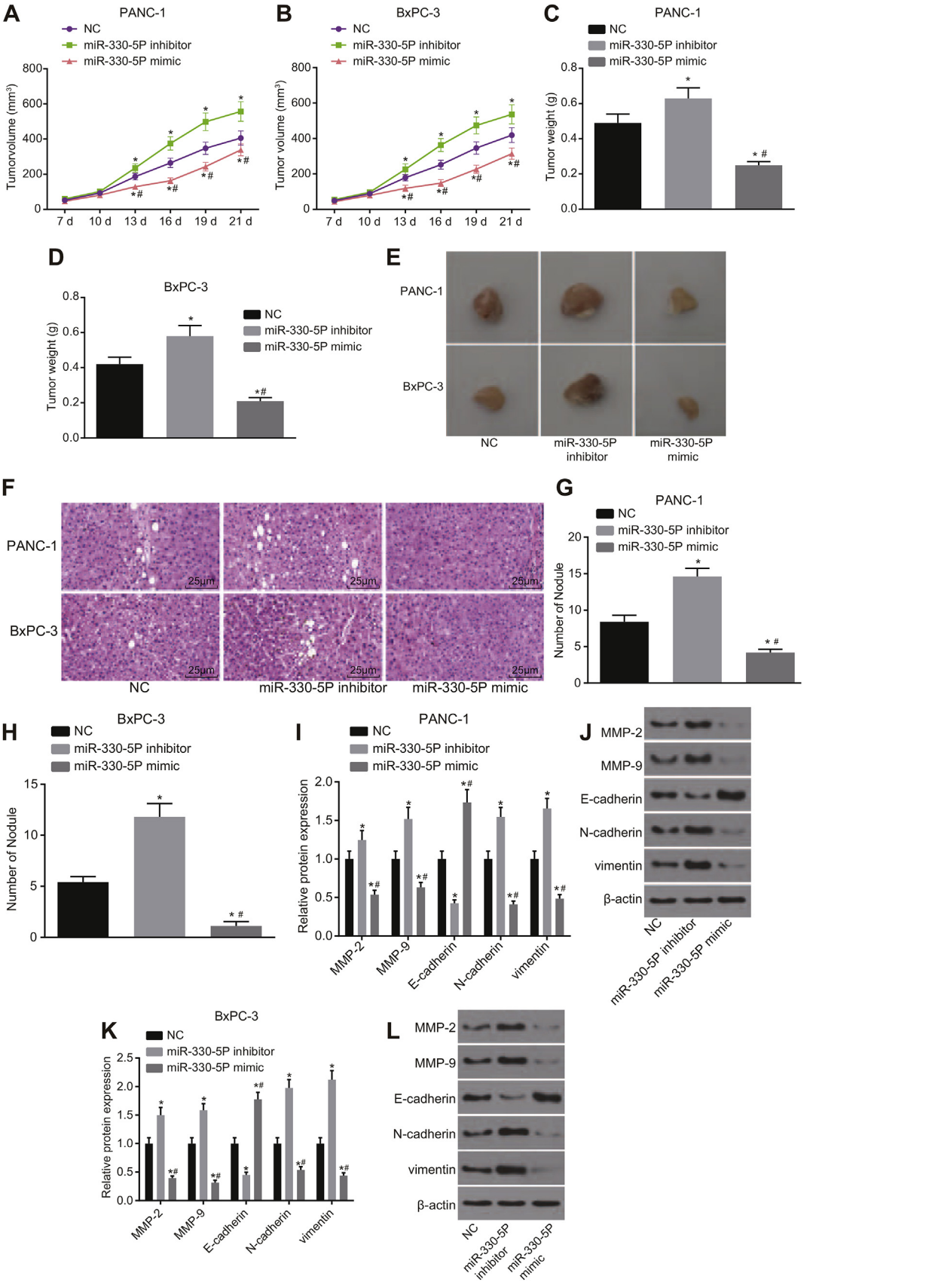

(caption on next page)

Fig. 5. Up-regulation of miR-330-5p inhibits invasion and metastasis of PC cells in nude mice. A&B, curve of tumor volume in nude mice injected with PANC-1 and BxPC-3 cells; C&D, curve of tumor weight in nude mice injected with PANC-1 and BxPC-3 cells on Day 21; F&G&H, the number of liver metastatic nodules in nude mice (400 ×) measured by HE staining; arrows represented nodule number; I&J, protein levels and protein bands of MMP-2, MMP-9, N-cadherin and vimentin in the liver metastatic nodules of miR-330-5p overexpression or inhibition PANC-1 cells; K&L, protein levels and protein bands of MMP-2, MMP-9, N-cadherin and vimentin in the liver metastatic nodules of miR-330-5p overexpression or inhibition BxPC-3 cells; the experiments were repeated 3 times and the measurement data were expressed as mean ± standard deviation; comparison among different groups were analyzed by using one-way analysis of variance; nude mice sample number n = 5; $^{*}, p < 0.05$, compared with the NC group; $^{\#}, p < 0.05$, compared with the miR-330-5p inhibitor group; PC, pancreatic cancer; NC, negative control; miR-330-5p, microRNA-330-5p; MMP, matrix metalloproteinase; PAX8, paired box 8; LINC00958, long intergenic non-coding 00958.

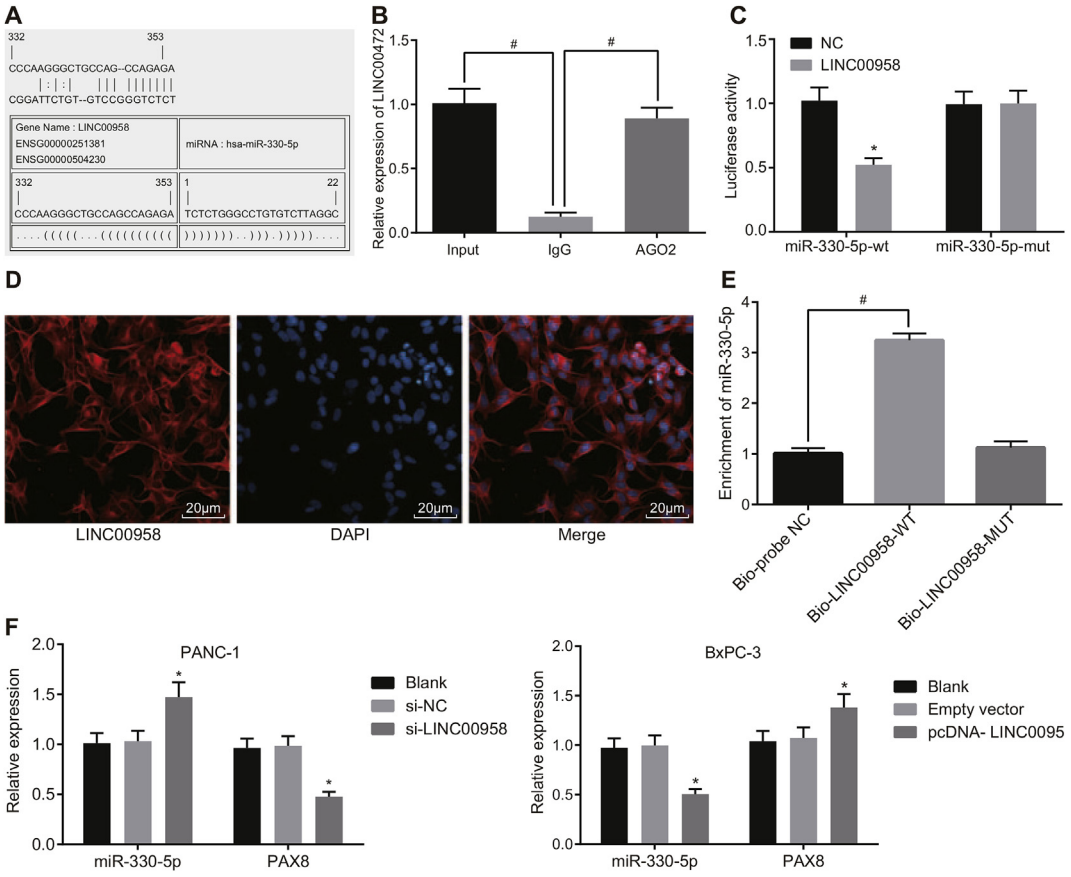

Fig. 6. LINC00958 could bind to miR-330-5p. A, prediction binding site of LINC00958 in miR-330-5p 3′UTR; B, LINC00958 could bind to AGO2 detected by using RIP; C, measurement of luciferase activity to verify the target relationship of LINC00958 with miR-330-5p; D, subcellular location of LINC00958 detected by FISH; E, relationship between LINC00958 and miR-330-5p detected by RNA pull down ($^{\#}, p < 0.05$, compared with Bio-probe NC); F, changes of expression of miR-330-5p and PAX8 after LINC00958 downregulation or overexpression; $^{*}, p < 0.05$, compared with the blank group; the above data were measurement data and expressed as mean ± standard deviation; comparison between two groups were analyzed by non-paired *t*-test, while comparison among different groups were analyzed by using one-way analysis of variance; the experiment was repeated 3 times; Wt, wild type; Mut, mutant type; NC, negative control; PC, pancreatic cancer; miR-330-5p, microRNA-330-5p; RIP, RNA immunoprecipitation; FISH, Fluorescent in Situ Hybridization; LINC00958, long intergenic non-coding 00958.

LINC00958 has direct interaction with AGO2 protein in PC cells. The results suggested that anti-AGO2 antibody could precipitate LINC00958, demonstrating LINC00958 could combine with AGO2 to form the complex. These results highlighted that the complex of LINC00958 and AGO2 could bind with miR-330-5p, resulting in a reduction in the dissociation of miR-330-5p (Fig. 6A, B, C).

Next, in order to detect whether LINC00958 could competitively combined with miR-330-5p to regulate PAX8, RNA pull down and FISH were performed to measure interaction between miR-330-5p and LINC00958 as well as subcellular location of LINC00958. The results of FISH (Fig. 6D) revealed that LINC00958 mainly expressed in the cytoplasm. The results of RNA pull down (Fig. 6E) showed that compared with the treatment of Bio-probe NC, the treatment of Bio-LINC00958-Wt significantly increased enrichment of miR-330-5p ($p < 0.05$), while no significant change was found in enrichment of miR-330-5p following the treatment of Bio-LINC00958-Mut ($p > 0.05$). Hence, LINC00958 could competitively sponge miR-330-5p and regulate its steady state.

Finally, to investigate the means by which LINC00958 regulates PAX8 expression by binding with miR-330-5p, the PANC-1 and BxPC-3 cells were treated with interference and overexpression LINC00958, with the blank group serving as the control. RT-qPCR was adopted to determine the expression of miR-330-5p and PAX8 in transfected cells, the results of which showed there to be no significant difference in relation to the PANC-1 cells regarding the expression of miR-330-5p and PAX8 between the blank and si-NC groups (all $p > 0.05$). Compared with the blank and si-NC groups, the si-LINC00958 group displayed significantly elevated miR-330-5p expression and significantly reduced PAX8 expression ($p < 0.05$). In the BxPC-3 cells, compared with the blank and empty vector groups, the pcDNA-LINC00958 group revealed significantly decreased miR-330-5p expression and significantly increased PAX8 expression ($p < 0.05$). These findings indicated that the downregulation of LINC00958 could inhibit the activation of the miR-330-5p/PAX8 axis by binding to miR-330-5p and repressing the expression of PAX8 resulting in the inhibition of

EMT, as well as the invasion and metastasis of PC cells (Fig. 6F).

4. Discussion

As an often fatal malignant tumor, at present PC has few effective therapeutic methods [30]. Reports have suggested the survival rate of PC to be as low as 4% within five years of diagnosis [1]. In recent years, accumulating evidence has demonstrated that lncRNAs are involved in various types of human cancers, including that of PC, playing central roles in the processes of tumor growth, cell invasion, metastasis, and apoptosis of PC cells [13]. However, the specific mechanism by which LINC00958 is associated with the processes of PC remains poorly understood. Therefore, the aim of the present study was to determine the modulatory effects of downregulation of LINC00958 on the EMT, invasion, and metastasis of PC cells via the regulation of miR-330-5p/PAX8 axis. Initially, our data obtained demonstrated that LINC00958 and PAX8 were upregulated and miR-330-5p was downregulated in PC cells. As a kind of oncogene, LINC00958 participates in regulation of the glioma tumorigenesis through mediating miR-203 and CDK2 [8]. A recent study has reported that LINC00958 expresses highly in bladder cancer and interacts with proteins related with initiation of translation and/or post-transcriptional modification of RNA to induce occurrence of malignancy, whose silencing reduces tumor cell survival ability and migration [14]. Interestingly, another study has proved that LINC00958 expression was upregulated in endometrial cancer [31]. A previous study revealed that lncRNAs were significantly upregulated in bladder cancer via the regulation of mRNA related pathways correlated with cellular movement [32]. Wang et al. asserted that lncRNA HOTTIP-005 and RP11-567G11.1 display elevated expression in patients with PC, which are widely considered to be poor prognostic factors closely associated with lymph node metastasis and overall survival [12]. Furthermore, in comparison to the adjacent normal pancreatic tissues, lncRNA MALAT1 exhibit higher expression levels in PC tissues, highlighting its potential as aprognostic indicator for PC [11] PAX8 has been identified as a new member of the PAX family expressed in the pancreas [33], with high expression of PAX8 considered to be a characteristic indicator of pancreatic primary tumors [20]. In specific terms, PAX8 could well serve as a prognostic marker in pancreatic endocrine tumors, with a loss in expression associated with malignant behavior [34]. In addition, miRs have been linked to a variety of cancers owing to their regulatory role in tumorigenesis influencing the expression levels of target genes [35]. Emerging evidences have revealed that some miRs are downregulated in PC tissues and cell lines [36]. For instance, downregulated miR-141 suppresses PC cell proliferation and invasion by targeting mitogen activated protein kinase isoform 4 (MAP4K4) [37].

The results of our study indicated that upregulation of miR-330-5p or silencing PAX8 reduced the expression of E-cadherin, MMP-2, and MMP-9 while elevating the expression of vimentin, suggesting that upregulation of miR-330-5p or silencing PAX8 can prevent EMT, invasion, and metastasis of PC cells. A significant quantity of literature has demonstrated that miRs play a vital role in a variety of biological processes, such as tumor EMT, invasion, and metastasis [38]. E-cadherin down-regulation and increased expression of mesenchymal proteins, including vimentin is considered to be molecular hallmarks of EMT [39]. Studies have suggested that miR-99a could increase expression of vimentin and reduce expression of E-cadherin so as to suppress EMT of PC cells [40]. Furthermore, up-regulation of MMP-2 and MMP-9 have been reported to be cell biomarkers of cell invasion [41], verifying that miR-218 represses migration and invasion of osteosarcoma cells, which are accompanied by down-regulated MMP2 and MMP9 [42]. Tréhoux et al. suggested that miR-330-5p could inhibit PC cell migration, invasion, and tumor growth by inhibiting the mucin 1 (MUC1) [19]. Moreover, the http://www.targetscan.org and dual-luciferase reporter gene assay validated that miR-330-5p targets and negatively modulates PAX8. PAX8 is also identified to exert effects on thyroid cancer [22]. S Li et al. reported that PAX2 induces EMT by reducing expression of E-cadherin [43]. Studies have revealed there to be a negative correlation between miR-375 and PAX6 that results in descended protein levels of MMP2 and MMP9, and ultimately repressing the migration and invasion of human breast cancer [44]. Based on these reports, we arrived at the conclusion that miR-330-5p overexpression could repress EMT, invasion, and metastasis of PC cells by negatively targeting PAX8.

Our results provided verification that LINC00958 could bind with miR-330-5p, and silencing LINC00958 can inhibit EMT, tumor growth, invasion, and metastasis of PC cells by suppressing the miR-330-5p/PAX8 axis. Consistent with our findings, a previous study indicated that HOTAIR knockdown inhibits tumor growth in mouse xenograft models of PC [45]. Interestingly, it has been demonstrated that LINC00958 exerts effects on carcinogensis in bladder cancer combined with modulation of pathways correlated with cellular movement and even cell death and survival [32]. Moreover, down-regulation of LINC00958 *in vitro* is reported to inhibit both cell invasion and migration [14]. Importantly, lncRNA MAP4K4 knockdown significantly suppresses PC cell growth with miR-141 overexpression [37], which supports the findings of the current study.

5. Conclusions

In conclusion, LINC00958 knockdown represses EMT, invasion, and metastasis of PC cells via the down-regulation of miR-330-5p/PAX8 axis (Fig. 7). Therefore, the identification of LINC00958 via miR-330-5p/PAX8 in PC cells may aid in facilitating the existing understanding of the mechanisms of PC, with potential of serving as a prognostic marker for the treatment of PC in the future. Further studies are required, however, to fully understand the specific mechanisms of LINC00958 combined with miR-330-5p/PAX8 axis on inhibition of EMT, invasion, and metastasis of PC cells.

Abbreviations

ANOVA, analysis of variance; BCA, bicinchoninic acid; ceRNA, competitive endogenous RNA; CI, confidence intervals; DAPI, 4′,6-diamidino-2-phenylindole; DEGs, differentially expressed genes; DMEM, Dulbecco modified Eagle medium; ECL, electro-chemi-luminescence; EMT, epithelial mesenchymal transition; FBS, fetal bovine serum; FDR, false positive discovery; HE, hematoxylin-eosin; HOTTIP, HOXA distal transcript antisense RNA; HR, hazard ratio; HRP, horseradish peroxidase; LINC00958, long intergenic noncoding RNA 00958; lncRNA, long noncoding RNA; MALAT-1, metastasis-associated lung adenocarcinoma transcript 1; MAP4K4, mitogenactivated protein kinase isoform; microRNA, miR; MMP, matrix metallopeptidase; mRNA, messenger RNA; MUC1, Mut, mucin 1; mutant; NC, negative control; PAGE, polyacrylamide gel electrophoresis; PAX, paired box; PC, pancreatic cancer; PVDF, polyvinylidene fluoride; RIP, RNA immunoprecipitation; RIPA, radio-immunoprecipitation assay; RT-qPCR, reverse transcription quantitative polymerase chain reaction; SDS, sodium dodecyl sulfate; UCA1, urothelial carcinoma-associated 1; Wt, wild type; 3'UTR, 3′ untranslated region.

Author contributions

S.C., J.Z.C., J.Q.Z., H.X.C., and F.N.Q. designed the study. S.C., M.L.Y., Y.F.T., and C.H.P. collated the data, designed and developed the database, carried out data analyses and produced the initial draft of the manuscript. B.Y.S., Y.L.C., and Y.D.W. contributed to drafting the manuscript. All authors have read and approved the final submitted manuscript.

Disclosure

S.C., J.Z.C., and J.Q.Z. contributed equally to this work. B.Y.S.,

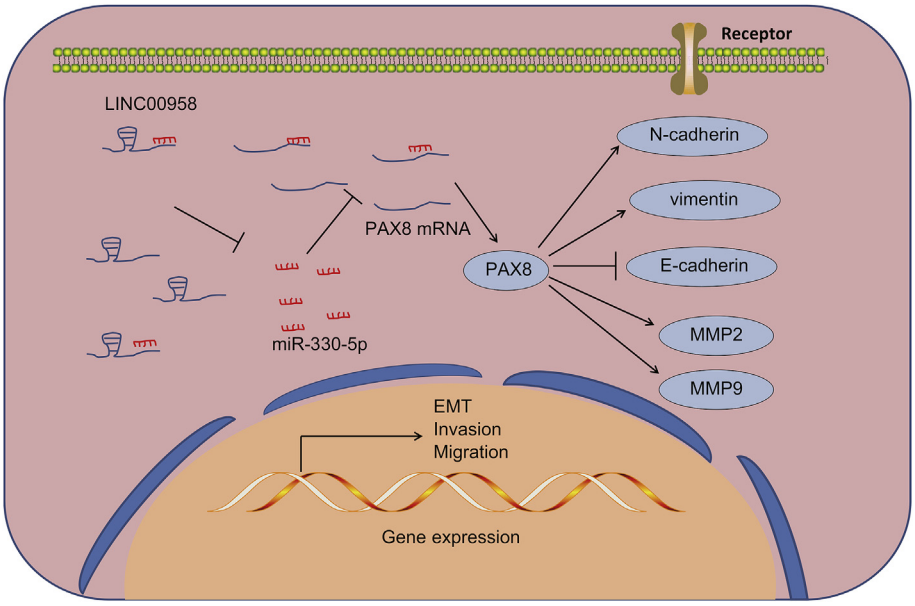

Fig. 7. Silencing LINC00958 represses EMT, invasion and metastasis of PC cells by inhibiting miR-330-5p/PAX8 axis. LINC00958 and PAX8 could bind with miR-330-5p. When LINC00958 was highly expressed in PC cells, the miR-330-5p that bound with NEK1 was decreased and PAX8 expression was increased. The expression of E-cadherin, MMP2, and MMP9 was upregulated, while expression of vimentin was decreased, and the EMT, invasion, and metastasis occurred in PC cells. When LINC00958 was downregulated, the miR-330-5p that bound with PAX8 was elevated, and PAX8 expression was decreased. The expression of E-cadherin, MMP2, and MMP9 was downregulated, while that of vimentin was elevated, and the EMT, invasion, and metastasis were inhibited in PC cells. PC, pancreatic cancer; miR-330-5p, microRNA-330-5p; MMP, matrix metalloproteinase; EMT, epithelial-mesenchymal transition; Nek1, NIMA-related protein kinase 1; PAX8, paired box 8; LINC00958, long intergenic non-coding 00958.

Y.L.C., and Y.D.W. also contributed equally, and all should be considered as co-corresponding author. The authors declare no conflicts of interest.

Acknowledgments

This study was supported in part by a grant from National Natural Science Foundation of China (#81772560 to Y.D. Wang, #81502008 to S. Chen, #81702438 to J.Z. Chen and #81802369 to J.Q. Zhang) and the Natural Science Foundation for Distinguished Young Scholars of Fujian Province (#2018J06020 to S. Chen).

References

[1] G.D. Batty, M. Kivimaki, D. Morrison, R. Huxley, G.D. Smith, R. Clarke, M.G. Marmot, M.J. Shipley, Risk factors for pancreatic cancer mortality: extended follow-up of the original Whitehall Study, Cancer Epidemiol. Biomark. Prev. 18 (2009) 673–675.
[2] A. Vincent, J. Herman, R. Schulick, R.H. Hruban, M. Goggins, Pancreatic cancer, Lancet 378 (2011) 607–620.
[3] S. Landi, Genetic predisposition and environmental risk factors to pancreatic cancer: a review of the literature, Mutat. Res. 681 (2009) 299–307.
[4] S. Raimondi, P. Maisonneuve, A.B. Lowenfels, Epidemiology of pancreatic cancer: an overview, Nat. Rev. Gastroenterol. Hepatol. 6 (2009) 699–708.
[5] L. Lei, J. Wang, L. Zhang, Y. Chen, P. Yuan, D. Liu, Meta-analysis of the clinical value of abnormally expressed long non-coding RNAs for pancreatic cancer, Oncotarget 8 (2017) 89149–89159.
[6] M. Hidalgo, Pancreatic cancer, N. Engl. J. Med. 362 (2010) 1605–1617.
[7] A. Cimadamore, S. Gasparrini, R. Mazzucchelli, A. Doria, L. Cheng, A. Lopez-Beltran, M. Santoni, M. Scarpelli, R. Montironi, Long non-coding RNAs in prostate cancer with emphasis on second chromosome locus associated with prostate-1 expression, Front. Oncol. 7 (2017) 305.
[8] E. Guo, C. Liang, X. He, G. Song, H. Liu, Z. Lv, J. Guan, D. Yang, J. Zheng, Long noncoding RNA LINC00958 accelerates gliomagenesis through regulating miR-203/CDK2, DNA Cell Biol. 37 (2018) 465–472.
[9] A. Kapinova, P. Kubatka, P. Zubor, O. Golubnitschaja, Z. Dankova, S. Uramova, I. Pilchova, M. Caprnda, R. Opatrilova, J. Richnavsky, P. Kruzliak, J. Danko, The hypoxia-responsive long non-coding RNAs may impact on the tumor biology and subsequent management of breast cancer, Biomed. Pharmacother. 99 (2018) 51–58.
[10] P. Chen, D. Wan, D. Zheng, Q. Zheng, F. Wu, Q. Zhi, Long non-coding RNA UCA1 promotes the tumorigenesis in pancreatic cancer, Biomed. Pharmacother. 83 (2016) 1220–1226.
[11] J.H. Liu, G. Chen, Y.W. Dang, C.J. Li, D.Z. Luo, Expression and prognostic significance of lncRNA MALAT1 in pancreatic cancer tissues, Asian Pac. J. Cancer Prev. 15 (2014) 2971–2977.
[12] Y. Wang, Z. Li, S. Zheng, Y. Zhou, L. Zhao, H. Ye, X. Zhao, W. Gao, Z. Fu, Q. Zhou, Y. Liu, R. Chen, Expression profile of long non-coding RNAs in pancreatic cancer and their clinical significance as biomarkers, Oncotarget 6 (2015) 35684–35698.
[13] X. Huang, X. Zhi, Y. Gao, N. Ta, H. Jiang, J. Zheng, LncRNAs in pancreatic cancer, Oncotarget 7 (2016) 57379–57390.
[14] A.K. Seitz, L.L. Christensen, E. Christensen, K. Faarkrog, M.S. Ostenfeld, J. Hedegaard, I. Nordentoft, M.M. Nielsen, J. Palmfeldt, M. Thomson, M.T. Jensen, R. Nawroth, T. Maurer, T.F. Orntoft, J.B. Jensen, C.K. Damgaard, L. Dyrskjot, Profiling of long non-coding RNAs identifies LINC00958 and LINC01296 as candidate oncogenes in bladder cancer, Sci. Rep. 7 (2017) 395.
[15] S.D. McAllister, R. Murase, R.T. Christian, D. Lau, A.J. Zielinski, J. Allison, C. Almanza, A. Pakdel, J. Lee, C. Limbad, Y. Liu, R.J. Debs, D.H. Moore, P.Y. Desprez, Pathways mediating the effects of cannabidiol on the reduction of breast cancer cell proliferation, invasion, and metastasis, Breast Canc. Res. Treat. 129 (2011) 37–47.
[16] T. Otsuki, M. Ishikawa, Y. Hori, G. Goto, A. Sakamoto, Volatile anesthetic sevoflurane ameliorates endotoxin-induced acute lung injury via microRNA modulation in rats, Biomed. Rep. 3 (2015) 408–412.
[17] Z.L. Ma, P.P. Hou, Y.L. Li, D.T. Wang, T.W. Yuan, J.L. Wei, B.T. Zhao, J.T. Lou, X.T. Zhao, Y. Jin, Y.X. Jin, MicroRNA-34a inhibits the proliferation and promotes the apoptosis of non-small cell lung cancer H1299 cell line by targeting TGFbetaR2, Tumour Biol. 36 (2015) 2481–2490.
[18] H.I. Yoo, B.K. Kim, S.K. Yoon, MicroRNA-330-5p negatively regulates ITGA5 expression in human colorectal cancer, Oncol. Rep. 36 (2016) 3023–3029.
[19] S. Trehoux, F. Lahdaoui, Y. Delpu, F. Renaud, E. Leteurtre, J. Torrisani, N. Jonckheere, I. Van Seuningen, Micro-RNAs miR-29a and miR-330-5p function as tumor suppressors by targeting the MUC1 mucin in pancreatic cancer cells, Biochim. Biophys. Acta 1853 (2015) 2392–2403.
[20] C.M. Haynes, A.R. Sangoi, R.K. Pai, PAX8 is expressed in pancreatic well-differentiated neuroendocrine tumors and in extrapancreatic poorly differentiated neuroendocrine carcinomas in fine-needle aspiration biopsy specimens, Canc. Cytopathol. 119 (2011) 193–201.
[21] M.P. Bartram, E. Amendola, T. Benzing, B. Schermer, G. de Vita, R.U. Muller, Mice lacking microRNAs in Pax8-expressing cells develop hypothyroidism and end-stage renal failure, BMC Mol. Biol. 17 (2016) 11.
[22] D. Wylie, S. Beaudenon-Huibregtse, B.C. Haynes, T.J. Giordano, E. Labourier, Molecular classification of thyroid lesions by combined testing for miRNA gene expression and somatic gene alterations, J. Pathol. Clin. Res. 2 (2016) 93–103.
[23] A. Fujita, J.R. Sato, O. Rodrigues Lde, C.E. Ferreira, M.C. Sogayar, Evaluating different methods of microarray data normalization, BMC Bioinf. 7 (2006) 469.
[24] G.K. Smyth, Linear models and empirical bayes methods for assessing differential expression in microarray experiments, Stat. Appl. Genet. Mol. Biol. 3 (2004) Article3.
[25] M.D. Robinson, D.J. McCarthy, G.K. Smyth, edgeR: a Bioconductor package for differential expression analysis of digital gene expression data, Bioinformatics 26 (2010) 139–140.
[26] P.J. Heagerty, Y. Zheng, Survival model predictive accuracy and ROC curves, Biometrics 61 (2005) 92–105.
[27] B. Liu, H. Yang, L. Taher, A. Denz, R. Grutzmann, C. Pilarsky, G.F. Weber, Identification of prognostic biomarkers by combined mRNA and miRNA expression microarray analysis in pancreatic cancer, Transl. Oncol. 11 (2018) 700–714.
[28] J. Yao, H.H. Cai, J.S. Wei, Y. An, Z.L. Ji, Z.P. Lu, J.L. Wu, P. Chen, K.R. Jiang, C.C. Dai, Z.Y. Qian, Z.K. Xu, Y. Miao, Side population in the pancreatic cancer cell lines SW1990 and CFPAC-1 is enriched with cancer stem-like cells, Oncol. Rep. 23 (2010) 1375–1382.
[29] Y. Wang, Y. Zhang, T. Yang, W. Zhao, N. Wang, P. Li, X. Zeng, W. Zhang, Long non-coding RNA MALAT1 for promoting metastasis and proliferation by acting as a ceRNA of miR-144-3p in osteosarcoma cells, Oncotarget 8 (2017) 59417–59434.
[30] A.V. Biankin, N. Waddell, K.S. Kassahn, M.C. Gingras, L.B. Muthuswamy, A.L. Johns, D.K. Miller, P.J. Wilson, A.M. Patch, J. Wu, D.K. Chang, M.J. Cowley, B.B. Gardiner, S. Song, I. Harliwong, S. Idrisoglu, C. Nourse, E. Nourbakhsh,

S. Manning, S. Wani, M. Gongora, M. Pajic, C.J. Scarlett, A.J. Gill, A.V. Pinho, I. Rooman, M. Anderson, O. Holmes, C. Leonard, D. Taylor, S. Wood, Q. Xu, K. Nones, J.L. Fink, A. Christ, T. Bruxner, N. Cloonan, G. Kolle, F. Newell, M. Pinese, R.S. Mead, J.L. Humphris, W. Kaplan, M.D. Jones, E.K. Colvin, A.M. Nagrial, E.S. Humphrey, A. Chou, V.T. Chin, L.A. Chantrill, A. Mawson, J.S. Samra, J.G. Kench, J.A. Lovell, R.J. Daly, N.D. Merrett, C. Toon, K. Epari, N.Q. Nguyen, A. Barbour, N. Zeps, I. Australian Pancreatic Cancer Genome, N. Kakkar, F. Zhao, Y.Q. Wu, M. Wang, D.M. Muzny, W.E. Fisher, F.C. Brunicardi, S.E. Hodges, J.G. Reid, J. Drummond, K. Chang, Y. Han, L.R. Lewis, H. Dinh, C.J. Buhay, T. Beck, L. Timms, M. Sam, K. Begley, A. Brown, D. Pai, A. Panchal, N. Buchner, R. De Borja, R.E. Denroche, C.K. Yung, S. Serra, N. Onetto, D. Mukhopadhyay, M.S. Tsao, P.A. Shaw, G.M. Petersen, S. Gallinger, R.H. Hruban, A. Maitra, C.A. Iacobuzio-Donahue, R.D. Schulick, C.L. Wolfgang, R.A. Morgan, R.T. Lawlor, P. Capelli, V. Corbo, M. Scardoni, G. Tortora, M.A. Tempero, K.M. Mann, N.A. Jenkins, P.A. Perez-Mancera, D.J. Adams, D.A. Largaespada, L.F. Wessels, A.G. Rust, L.D. Stein, D.A. Tuveson, N.G. Copeland, E.A. Musgrove, A. Scarpa, J.R. Eshleman, T.J. Hudson, R.L. Sutherland, D.A. Wheeler, J.V. Pearson, J.D. McPherson, R.A. Gibbs, S.M. Grimmond, Pancreatic cancer genomes reveal aberrations in axon guidance pathway genes, Nature 491 (2012) 399–405.

[31] B.J. Chen, F.L. Byrne, K. Takenaka, S.C. Modesitt, E.M. Olzomer, J.D. Mills, R. Farrell, K.L. Hoehn, M. Janitz, Transcriptome landscape of long intergenic non-coding RNAs in endometrial cancer, Gynecol. Oncol. 147 (2017) 654–662.

[32] A. Atala, Re: profiling of long non-coding RNAs identifies LINC00958 and LINC01296 as candidate oncogenes in bladder cancer, J. Urol. 198 (2017) 983–985.

[33] P.I. Lorenzo, C.M. Jimenez Moreno, I. Delgado, N. Cobo-Vuilleumier, R. Meier, L. Gomez-Izquierdo, T. Berney, R. Garcia-Carbonero, A. Rojas, B.R. Gauthier, Immunohistochemical assessment of Pax8 expression during pancreatic islet development and in human neuroendocrine tumors, Histochem. Cell Biol. 136 (2011) 595–607.

[34] K.B. Long, A. Srivastava, M.S. Hirsch, J.L. Hornick, PAX8 Expression in well-differentiated pancreatic endocrine tumors: correlation with clinicopathologic features and comparison with gastrointestinal and pulmonary carcinoid tumors, Am. J. Surg. Pathol. 34 (2010) 723–729.

[35] E.J. Lee, Y. Gusev, J. Jiang, G.J. Nuovo, M.R. Lerner, W.L. Frankel, D.L. Morgan, R.G. Postier, D.J. Brackett, T.D. Schmittgen, Expression profiling identifies microRNA signature in pancreatic cancer, Int. J. Canc. 120 (2007) 1046–1054.

[36] S. Yu, Z. Lu, C. Liu, Y. Meng, Y. Ma, W. Zhao, J. Liu, J. Yu, J. Chen, miRNA-96 suppresses KRAS and functions as a tumor suppressor gene in pancreatic cancer, Cancer Res. 70 (2010) 6015–6025.

[37] G. Zhao, B. Wang, Y. Liu, J.G. Zhang, S.C. Deng, Q. Qin, K. Tian, X. Li, S. Zhu, Y. Niu, Q. Gong, C.Y. Wang, miRNA-141, downregulated in pancreatic cancer, inhibits cell proliferation and invasion by directly targeting MAP4K4, Mol. Canc. Therapeut. 12 (2013) 2569–2580.

[38] X.M. Ding, MicroRNAs: regulators of cancer metastasis and epithelial-mesenchymal transition (EMT), Chin. J. Canc. 33 (2014) 140–147.

[39] Y. Sun, L. Hu, H. Zheng, M. Bagnoli, Y. Guo, R. Rupaimoole, C. Rodriguez-Aguayo, G. Lopez-Berestein, P. Ji, K. Chen, A.K. Sood, D. Mezzanzanica, J. Liu, B. Sun, W. Zhang, MiR-506 inhibits multiple targets in the epithelial-to-mesenchymal transition network and is associated with good prognosis in epithelial ovarian cancer, J. Pathol. 235 (2015) 25–36.

[40] D. Li, X. Li, W. Cao, Y. Qi, X. Yang, Antagonism of microRNA-99a promotes cell invasion and down-regulates E-cadherin expression in pancreatic cancer cells by regulating mammalian target of rapamycin, Acta Histochem. 116 (2014) 723–729.

[41] W.C. Hung, W.L. Tseng, J. Shiea, H.C. Chang, Skp2 overexpression increases the expression of MMP-2 and MMP-9 and invasion of lung cancer cells, Cancer Lett. 288 (2010) 156–161.

[42] J. Jin, L. Cai, Z.M. Liu, X.S. Zhou, miRNA-218 inhibits osteosarcoma cell migration and invasion by down-regulating of TIAM1, MMP2 and MMP9, Asian Pac. J. Cancer Prev. 14 (2013) 3681–3684.

[43] L. Li, Y. Wu, Y. Yang, Paired box 2 induces epithelial-mesenchymal transition in normal renal tubular epithelial cells of rats, Mol. Med. Rep. 7 (2013) 1549–1554.

[44] Q. Zou, W. Yi, J. Huang, F. Fu, G. Chen, D. Zhong, MicroRNA-375 targets PAX6 and inhibits the viability, migration and invasion of human breast cancer MCF-7 cells, Exp. Ther. Med. 14 (2017) 1198–1204.

[45] K. Kim, I. Jutooru, G. Chadalapaka, G. Johnson, J. Frank, R. Burghardt, S. Kim, S. Safe, HOTAIR is a negative prognostic factor and exhibits pro-oncogenic activity in pancreatic cancer, Oncogene 32 (2013) 1616–1625.